29. Quitterer U, Hoffmann M, Freichel M et al. Paradoxical block of parathormone secretion is mediated by increased activity of G alpha subunits. J Biol Chem 2001; 276: 6763–6769
30. Miki H, Maercklein PB, Fitzpatrick LA. Effect of magnesium on parathyroid cells: evidence for two sensing receptors or two intracellular pathways? Am J Physiol 1997; 272: E1–E6
31. Rodriguez ME, Almaden Y, Cañadillas S et al. The calcimimetic R-568 increases vitamin D receptor expression in rat parathyroid glands. Am J Physiol Renal Physiol 2007; 292: F1390–F1395
32. Ben-Dov IZ, Galitzer H, Lavi-Moshayoff V et al. The parathyroid is a target organ for FGF23 in rats. J Clin Invest 2007; 117: 4003–4008

Paracrine effects of transplanted mesothelial cells isolated from temperature-sensitive SV40 large T-antigen gene transgenic rats during peritoneal repair

Reo Kanda, Chieko Hamada, Kayo Kaneko, Takanori Nakano, Keiichi Wakabayashi, Kazuaki Hara, Hiroaki Io, Satoshi Horikoshi and Yasuhiko Tomino

Division of Nephrology, Department of Internal Medicine, Faculty of Medicine, Juntendo University, Tokyo, Japan

Correspondence and offprint requests to: Yasuhiko Tomino; E-mail: yasu@juntendo.ac.jp

ABSTRACT

Background. The prevention and restoration of peritoneal damage is a critical mission in peritoneal dialysis (PD). Transplantation of mesothelial cells has been suggested to suppress peritoneal injury during PD. Few studies have examined the efficacy and safety of cell transplantation. We evaluated the paracrine effects of mesothelial transplantation during peritoneal repair using immortalized temperature-sensitive mesothelial cells (TSMCs) in chlorhexidine gluconate (CG)-induced peritoneal fibrosis rats.

Methods. Continuous-infusion pumps containing 8% CG were placed into the abdominal cavity for 21 days. After the removal of the pumps, the TSMCs were injected into the peritoneal cavity at Day 22 (Tx-1 group) or 29 (Tx-2 group). Morphological findings and mRNA expressions of regeneration-related factors were examined at Days 22, 29 and 35.

Results. Peritoneal thickness was aggravated in the Tx-1 group. Levels of transforming growth factor (TGF)-β, vascular endothelial growth factor (VEGF) and matrix metalloproteinase-2 mRNA in the Tx-1 group at Day 35 were comparable with those at Day 22. The levels of Snail, B-Raf and ERK-1, markers of epithelial to mesenchymal transition and of the RAS/MAPK pathway in the Tx-1 group, were significantly higher than those in the Tx-2 group. TGF-β and VEGF were produced from the transplanted mesothelial cells and the surrounding cells in the Tx-1 group.

Conclusion. It appears that the paracrine effect of transplanted mesothelial cells during peritoneal repair is associated with its surrounding condition. It is important to determine the most appropriate time for developing peritoneal repair through mesothelial transplantation.

Keywords: EPS, mesothelial cells, peritoneal dialysis, peritoneal injury, transplantation

INTRODUCTION

Peritoneal dialysis (PD) is a common renal replacement therapy for patients with end-stage kidney disease, and the preservation of residual kidney function and the high quality of life are advantages of PD treatment. The peritoneal membrane is lined by a monolayer of mesothelial cells that have some of the characteristics of epithelial cells, act as a permeability barrier, and secrete various substances involved in the regulation of peritoneal permeability and local host defense [1–3]. Long-term exposure to the hyperosmotic,

hyperglycemic and acidic solutions used in dialysis often causes persistent inflammation and injury to the peritoneum, which progressively becomes denuded of mesothelial cells and undergoes fibrosis [4, 5].

Mesothelial cells have been shown to play a central role in peritoneal homeostasis and immunoregulation [6]. Various studies have focused on the potential use of mesothelial cells in gene therapy and cell transplantation, both of which may provide novel therapeutic strategies for the preservation of the peritoneum during in PD [6–9]. Previous reports suggest that cultured mesothelial cells have been able to change their morphological features and produce extracellular matrix components in response to various stimuli [10, 11]. Mesothelial cells cultured with mediums containing high concentrations of glucose or inflammatory cytokines expressed high transforming growth factor β (TGF-β) and snail mRNA [12, 13]. However, it is notable that, depending on the surrounding environment, the transplanted mesothelial cells have been a double-edged sword, switching from an epithelial phenotype that contributes to the resolution of peritoneal injury and inflammation to an invasive, migratory and activated mesenchymal phenotype that contributes to neoangiogenesis, fibrosis and peritoneal dysfunction. The relevance of the pro-fibrotic growth factor TGF-β in the failure of ultrafiltration induced by PD was underscored in a rat model in which the TGF-β gene was transduced to the peritoneum, where it was associated with a decrease in peritoneal function [14]. We established temperature-sensitive immortalized mesothelial cell (TSMC) lines, which are not proliferated but only differentiated at 38°C or more such as peritoneal cavity, from temperature-sensitive SV40 large T antigen gene transgenic rats [15]. The repeatedly subcultured mesothelial cells are retaining the characteristics of primary mesothelial cell [15]. The mesothelial cells transplanted into the peritoneal cavity play a role in peritoneal homeostasis and immunoregulation without their proliferation. To examine the paracrine effect of transplanted mesothelial cells, which synthesize cytokines and growth factors, the peritoneal mesothelial cells were injected into the peritoneal cavity in CG-induced peritoneal fibrosis rats at various times.

MATERIALS AND METHODS

Rats

Forty-five male Sprague-Dawley rats (200–250 g body weight at the age of 8 weeks) were housed under conventional laboratory conditions of a constant 22°C temperature with a 12 h light/dark cycle. They had free access to laboratory chow and tap water in standard rodent cages. The experimental protocols were approved by the Ethics Review Committee for Animal Experimentation at Juntendo University Faculty of Medicine, Tokyo, Japan.

Peritoneal fibrosis animal models

Eight percent chlorhexidine gluconate (CG) in 15% ethanol was dissolved in 2-mL distilled water within continuous-infusion pumps with an infusion rate of 2.5 µL/h, according to the previous report [16]. Under ether anesthesia, each infusion pump was placed in the lower abdominal cavity of a rat with the exit oriented in the caudal direction for 21 days. As a control, 15% ethanol was dissolved in 2-mL distilled water within the infusion pumps and each infusion pump was placed in the lower abdominal cavity of a rat for 21 days. The continuous-infusion pumps were removed at Day 21. The anterior abdominal peritoneum was obtained at Days 0, 22, 29, and 35.

Preparation of mesothelial cell lines

We established TSMC lines from temperature-sensitive SV40 large T antigen gene transgenic rats [15]. TSMCs progressively grow at 33°C, and are suspended and differentiated at 38°C, whereas the cells are continuously sustaining the native morphological and functional characteristics of primary mesothelial cells. The pIRES2-EGFP vector was constructed and transfected into the TSMCs using Lipofectamine 2000 (Invitrogen, Carlsbad, CA, USA) according to the manufacturer's protocols [17]. Green fluorescent protein (GFP) expressing TSMCs were selected by Geneticin (1 mg/mL).

TSMCs were cultured on the surface of temperature-responsive culture dishes covalently bonded with the thermally sensitive polymer, poly (N-isopropylacrylamide) with M199 medium (Invitrogen Co., Tokyo, Japan) containing 10% fetal calf serum (FCS), 10 U/mL, penicillin and 100 µg/mL streptomycin at 33°C in an incubator. After the cells reached confluence, they were harvested from these dishes by reducing the temperature (from 33 to 20°C) retaining cell–cell junctions and basement membranes.

Administration of TSMCs in CG-induced peritoneal fibrosis rats

After the removal of the infusion pumps at Day 21, the TSMCs (1×10^6 cells/1 mL/100 g body weight) were injected into the peritoneal cavity of the peritoneal fibrosis rats at Day 22 (Tx-1 group) or 29 (Tx-2 group). The anterior abdominal peritoneum was obtained at Day 35. The peritoneal samples were immediately fixed in a 20% formaldehyde solution and then embedded in paraffin. Then, 4-µm sections were prepared and stained with Masson's trichrome. Histological assessment was performed using the Imaging System KS400 (Kontron Elektronik GmbH, Eching, Germany).

Histological analysis

The thickness of the submesothelial compact (SMC) zone, which is a submesothelial interstitial layer between the mesothelial surface and the upper border of peritoneal adipose tissues, was measured as peritoneal fibrosis. In accordance with a previous report [18], the maximum thickness of the SMC zone was measured in each section-oriented perpendicular to the serosal surface in micrometers. Five portions were randomly selected for the measurement of submesothelial thickness. The thickness was measured using the Imaging System KS400 [19], and then the average peritoneal thickness was calculated for each specimen. Vascular density in the peritoneum (number/SMC mm^2) at 10 random areas in each tissue was counted by immunohistochemistry using a mouse anti-rat CD31 antibody (Thermo Scientific, Waltham, USA), and the average vascular density was calculated using the Imaging System KS400.

Immunohistochemistry

All sections were deparaffinized in xylene, followed by 100% ethanol and then placed in a freshly prepared methanol/0.3% H_2O_2 solution for 15 min to block the endogenous peroxidase activity. Microwave antigen retrieval was performed with a hot 0.01 mol/L citrate buffer for 20 min. The sections were cooled to room temperature before performing subsequent procedures, and then blocked by a blocking solution containing 2% bovine serum albumin (BSA), 2% FCS and 0.2% fish gelatin in 0.01 mol/L PBS (pH 7.4) for 30 min, followed by overnight incubation with a rabbit anti-mouse GFP antibody diluted to 1:200 (FRL, Hokkaido, Japan) to detect the TSMCs, a rabbit anti-rat monocyte chemotactic protein-1 (MCP-1) antibody diluted to 1:100 (Abcam, Cambridge, UK), which reacts with infiltrating monocytes and basophils, and a rabbit anti-rat vimentin antibody diluted to 1:250 (Abcam, Cambridge, UK), which reacts with mesenchymal cells at 4°C. The sections for GFP, MCP-1 and vimentin immunostaining were incubated with a polyclonal goat anti-rabbit antiserum conjugated with peroxidase (Histofine Simple Stain MAX-PO, Nichirei Biosciences, Tokyo, Japan) at room temperature for 30 min. The bound antibodies were visualized with 3, 3′-diaminobenzine containing 0.003% H_2O_2. The negative control was confirmed by incubation without primary or secondary antibodies to show no positive cells. The sections were washed with PBS (pH 7.4) three times after each incubation, except before the addition of the primary antibodies. All sections were counterstained with Mayer's hematoxylin at room temperature for 3 min before mounting with a Glycergel mounting medium (MOUNT-QUICK, Daido Sangyo, Saitama, Japan). The objective (×100) was positioned at random on the section. The number of GFP, MCP-1 or vimentin-positive cells in the peritoneum at 10 random areas in each tissue was counted, and the average number of cells was calculated (the number of GFP, MCP-1 or vimentin-positive cells/SMC mm^2).

Double immunofluorescence

All sections were deparaffinized in xylene, followed by 100% ethanol. Thereafter, microwave antigen retrieval was performed with hot 0.01 mol/L citrate buffer for 20 min. The sections were cooled to room temperature before performing subsequent procedures, and then blocked by a blocking solution containing 2% BSA, 2% FCS and 0.2% fish gelatin in 0.01 mol/L PBS (pH 7.4) for 30 min, followed by overnight incubation with a rabbit anti-mouse GFP antibody diluted to 1:40 (FRL, Hokkaido, Japan) to detect the TSMCs. After the GFP enhancement step, the sections were washed in PBS to stop the reaction and incubated again with a mouse anti-rat alpha-smooth muscle actin (α-SMA) antibody diluted to 1:40 (Abcam, Cambridge, MA, USA), which reacts with fibroblasts, a mouse anti-rat TGF-β antibody diluted to 1:40 (Abcam, Cambridge, UK), a mouse anti-rat vascular endothelial growth factor (VEGF) antibody diluted to 1:50 (Abcam, Cambridge, UK).

After overnight incubation at 4°C, the sections were washed in PBS and mounted in diluted Alexa 488 green or Alexa 555 red as a secondary antibody at room temperature for 60 min.

Negative controls were performed by omitting primary antibodies. In all fluorescent images cell nuclei were labeled with a DAPI stain.

Quantitative real-time PCR

Total RNA was extracted from peritoneal specimens using a trizol reagent (Invitrogen AG, Basel, Switzerland) and the RNeasy Mini Kit (Qiagen K.K., Tokyo, Japan). The RNA quantity was assessed using a NanoDrop ND-1000 spectrophotometer (NanoDrop Products, Wilmington, DE, USA). A 16 µL reaction mixture containing 1 µg of RNA, 4 µL of 2.5 mmol/L dNTP mixture (Takara Biochemicals, Ohtsu, Japan) and 2 µL of Random Decamers RETROscript (Ambion, Inc., Austin, TX, USA) in RNase-free water was inactivated by heating at 70°C for 3 min. The product was added to 2 µL of 10× polymerase chain reaction (PCR) buffer (Takara Bio, Inc., Shiga, Japan), 1 µL of Protector RNase Inhibitor (Roche Diagnostics Corp., Mannheim, Germany) and 0.5 µL of M-MLV Reverse Transcriptase (Invitrogen Corp., Carlsbad, CA, USA), followed by incubation at 42°C for 60 min. The complementary DNA (cDNA) product was used for real-time PCR. A 2 µL aliquot of diluted cDNA, 1.6 µL forward primers, 1.6 µL reverse primers, 10 µL SYBR Green PCR Master Mix (Applied Biosystems, Carlsbad, CA, USA) and 4.8 µL of cDNA-free double-distilled water were then mixed to obtain a final reaction mixture of 20 µL according to the manufacturer's instructions. The mixture was denatured and amplified using a 7500 Real-Time PCR system (Applied Biosystems) under the following conditions: (i) 20 s at 95°C for 1 cycle, (ii) 3 s at 95°C and 30 s at 60°C for 40 cycles, (iii) 15 s at 95°C, 60 s at 60 °C, 15 s at 95°C and 15 s at 60°C for 1 cycle. The cDNA-free double-distilled water as a negative control was included in each reaction. For the quantification of the PCR product, the samples were standardized with the PCR product for glyceraldehydes-3- phosphate dehydrogenase. The PCR primers were designed as follows: TGF-β, 5′-ATGGTGGACCGCAACAA CGCAAT-3′ (forward) and 5′-CAGCTCTGCACGGGACAG CAAT-3′ (reverse); VEGF, 5′-ACTGGACCCTGGCTTTACTG CTG-3′ (forward) and 5′-TTCACCACTTCATGGGCTTTCT GCT-3′ (reverse); MMP-2, 5′-TGCAGGGTGGTGGTCACAG CTA-3′ (forward) and 5′-AGCAGCCCAGCCAGTCCGATT T-3′ (reverse); HGF, 5′-GGCTGGGGCTACACTGGATTGAT-3′ (forward) and 5′-TTGCCTTGATGGTGCTGACTGC-3′ (reverse); PAI-1, 5′-GGCGTCTTCCTCCACAGCCATT-3′ (forward) and 5′-TCCCACTCTCAAGGCTCCATCAGC-3′ (reverse); MCP-1, 5′-AGGTCTCTGTCACGCTTCTGGG-3′ (forward) and 5′-TA GCAGCAGGTGAGTGGGGCAT-3′ (reverse); vimentin, 5′-CC AGGCAAAGCAGGAGTCAAACG-3′ (forward) and 5′-TCTT CCATTTCACGCATCTGGCG-3′ (reverse); B-Raf, 5′-GTGGG GATGGAGCCCCTTTGAA-3′ (forward) and 5′-ACACTGGG CCAGGCTCAAAATCA-3′ (reverse); MEK-1, 5′-TTGGGGTC AGCGGGCAGCTAAT-3′ (forward) and 5′-GGAGTCTCT CAGGCGACATGTAGGA-3′ (reverse); ERK-1, 5′-CAACAC CACCTGCGACCTTA-3′ (forward) and 5′-TTGGTGTAGCC CTTGGAGTT-3′ (reverse); Snail, 5′-ACAGCGAACTGGA CACACACACA-3′ (forward) and 5′-AGGGGAGTGGAATG GAACTGCTGA-3′ (reverse).
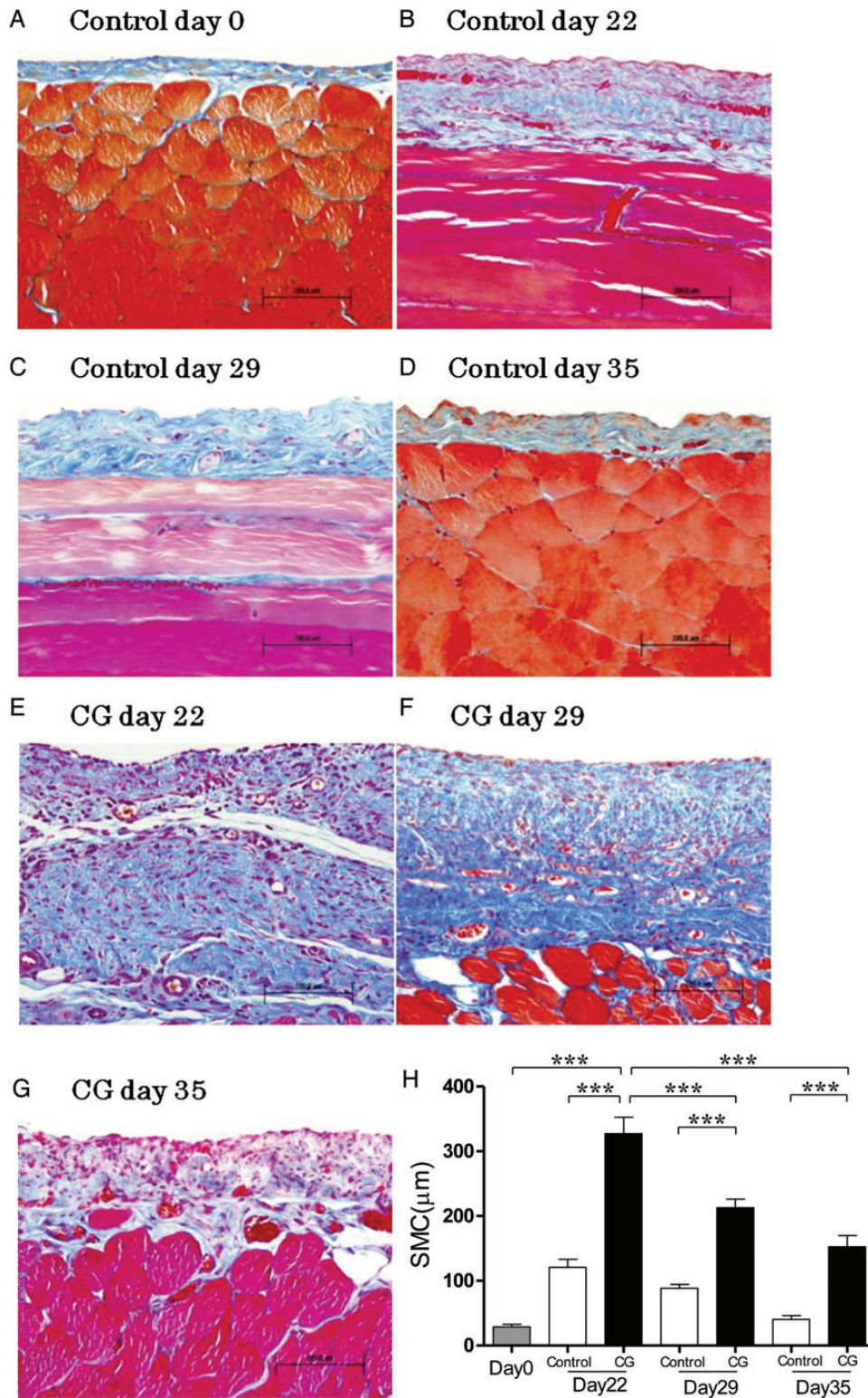
FIGURE 1: Histological features of the anterior abdominal wall (Masson's trichrome staining, ×200, $n = 5$ in each group). (**A**) Rat at day 0. (**B**) Rat stimulated with 15% ethanol for 21 days at Day 22. (**C**) Rat stimulated with 15% ethanol for 21 days at Day 29. (**D**) Rat stimulated with 15% ethanol for 21 days at Day 35. (**E**) Rat stimulated with 8% CG for 21 days at Day 22. (**F**) Rat stimulated with 8% CG for 21 days at Day 29. (**G**) Rat stimulated with 8% CG for 21 days at Day 35. (**H**) Average thickness of SMC increased with time during continuous stimulation of CG, and then decreased after cessation of CG. Error bars represent SD.

Statistical analysis

The data are expressed as means ± SD. Differences between groups were examined for statistical significance using one-way analysis of variance. Statistical analysis was performed with the Graph Pad PRISM Version 5.0 software. Differences at $P < 0.05$ were considered significant.

Serial morphological changes of interstitium

In the control group, the peritoneal tissue consisted of a peritoneal mesothelial monolayer and thin connective tissues under the mesothelial layer at Day 0 (Figure 1A). The SMC thickening introduced by ethanol diluted distilled water decreased at Day 35 in the control group (Figure 1B–D). CG enhanced morphological alteration and cell infiltration compared with the control (Figure 1E). At 14 days after cessation of CG stimulation, the marked regressions of submesothelial thickening and cell infiltration were observed (Figure 1F and G). Diluted ethanol increased the thickness of SMC at Day 22 in the control, then the thickness entirely recovered at Day 35 (Figure 1H). Although the increase of SMC thickening caused by continuous CG exposure was attenuated with the time of the cessation of CG, the thickness of SMC was not restored to its former thickness until Day 35 (Figure 1H) in the CG group. The mesothelial cells were observed on the surface of the peritoneum (Figure 1A–H) in the control and CG group. In the peritoneum, the levels of TGF-β and VEGF mRNAs at Day 22 were significantly higher than those at Day 29 (Figure 2F and G).
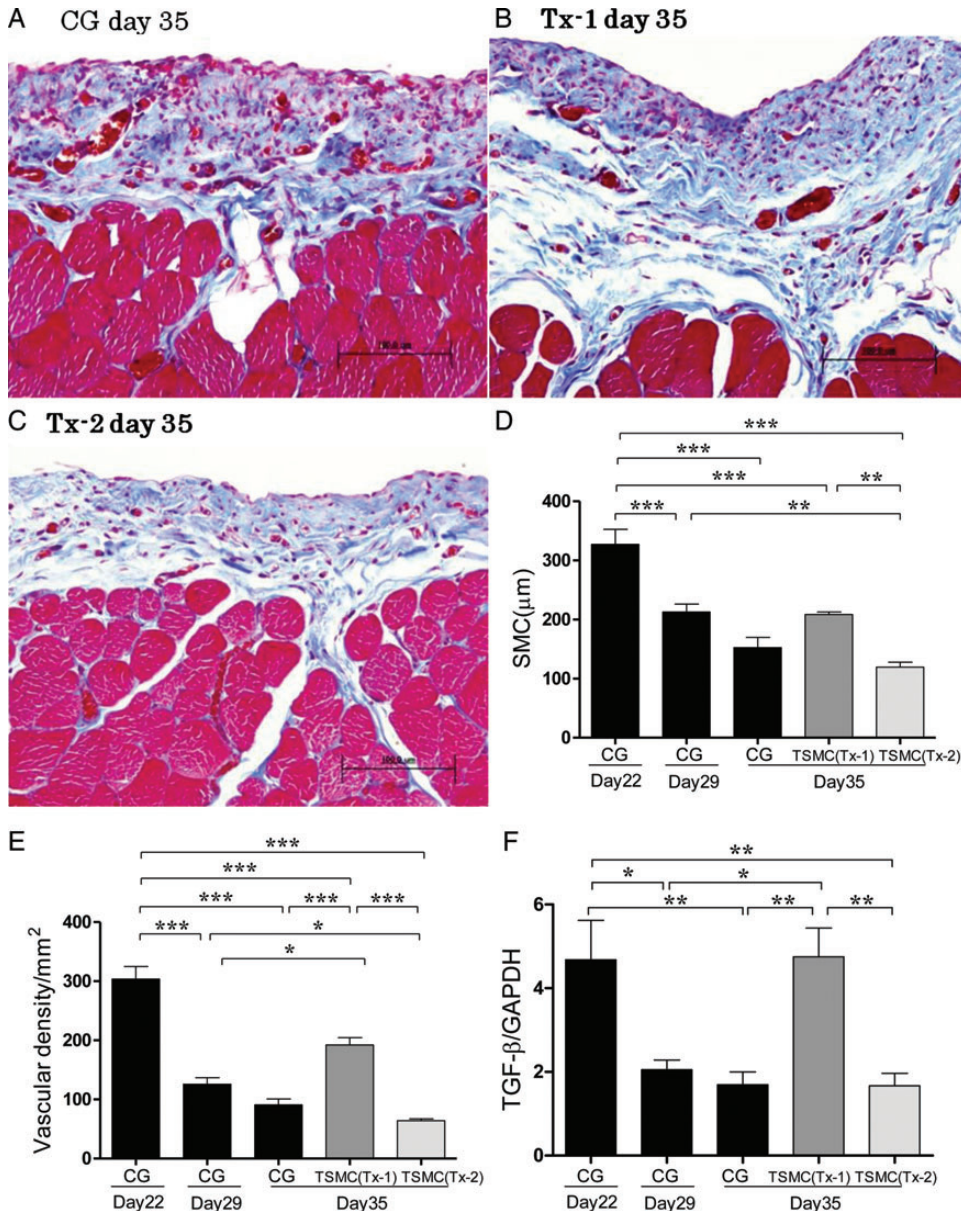
FIGURE 2: At Day 35, histological features of the anterior abdominal wall (Masson's trichrome staining, ×200, $n = 5$ in each group). (**A**) Rat stimulated with 8% CG for 21 days (CG group). (**B**) Rat stimulated with 8% CG for 21 days and treated with TSMCs at Day 22 (Tx-1 group). (**C**) Rat stimulated with 8% CG for 21 days and treated with TSMCs at Day 29 (Tx-2 group). (**D**) Average thickness of SMC at day 35 was aggravated in the Tx-1 group. Average thickness of SMC at Day 35 was no difference between the CG group and Tx-2 group. (**E**) Average vascular density at Day 35 was aggravated in the Tx-1 group. Average vascular density at Day 35 was no difference between the CG group and Tx-2 group. (**F and G**) At Day 35, the levels of TGF-β and VEGF mRNA expression remained high in the Tx-1 group. (**H**) At Day 35, the level of matrix metalloproteinase-2 mRNA expression was significantly higher in the Tx-1 group. (**I and J**) At Day 35, the levels of HGF and PAI-1 mRNA expression were not significant changes. Error bars represent SD.
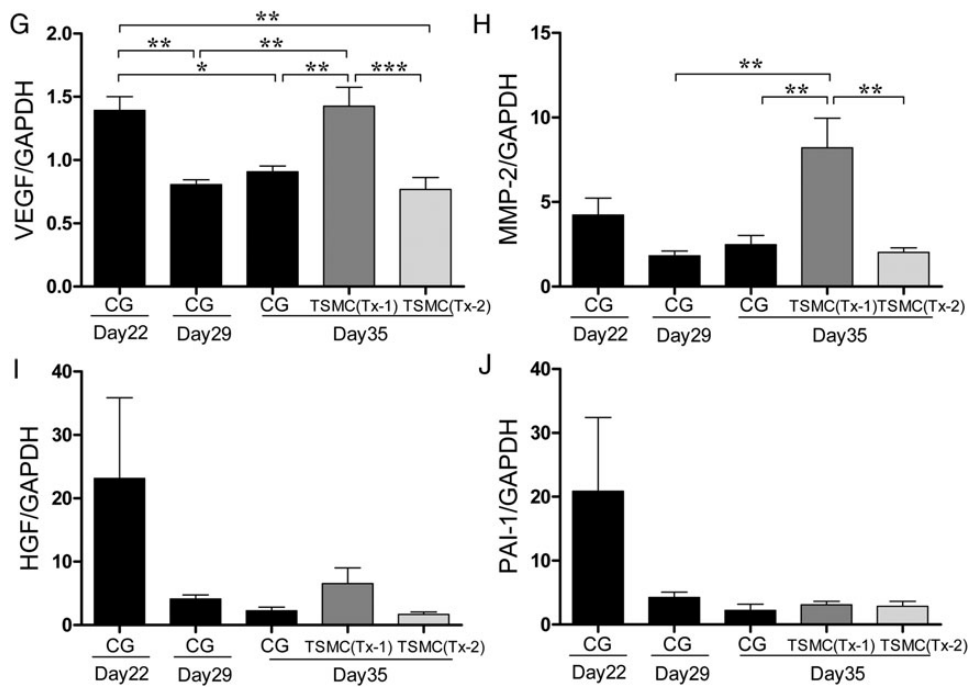
FIGURE 2: *Continued*

Morphological changes and mRNA expressions of the regeneration-related factors after TSMCs transplantation

In the CG group at Day 35, the peritoneal tissues consisted of SMC thickening, numerous mononuclear cell infiltration, angiogenesis and a substantial loss of mesothelial cells (Figure 2A). In the Tx-1 group at Day 35, the peritoneal tissues consisted of the progressive SMC thickening, numerous mononuclear cells and partial loss of mesothelial cells (Figure 2B). SMC thickness and degree of interstitial cells, such as mononuclear cells and mesothelial cells, in the Tx-2 group at Day 35 were comparable with those in the CG group at Day 35 (Figure 2C). TSMC transplantation at Day 22 (Tx-1 group) aggravated the SMC thickening and angiogenesis. TSMC transplantation at Day 29 (Tx-2 group) had no significant effect in the peritoneal repair (Figure 2D and E).

In real-time PCR analysis, the expressions of TGF-β and VEGF mRNA at Day 35 in the Tx-1 group were comparable with those at Day 22 in the CG group (Figure 2F and G). The level of matrix metalloproteinase-2 (MMP-2) mRNA expression at Day 35 in the Tx-1 group was significantly higher than that at Day 35 in the CG and the Tx-2 group (Figure 2H). The levels of HGF, PAI-1 mRNA expression did not have significant changes (Figure 2I and J).

Analysis of interstitial cells at Day 35
Appearance of GFP-positive TSMCs. TSMCs were transfected GFP before administration into peritoneal cavity. There were no GFP-positive cells in the CG group at Day 35 (Figure 3A). No GFP-positive cells were detected in the mesothelial cells on the surface of the peritoneum in both Tx-1 and Tx-2 groups. However, the GFP-expressing TSMCs were observed in the thickened SMC (Figure 3B and C). Some of

GFP-positive TSMCs appeared spindle-shape, such as fibroblasts and epithelial to mesenchymal transition (EMT) mesothelial cells in the peritoneum. The number of GFP-positive cells was not different between the Tx-1 group and Tx-2 group (Figure 3D).

Appearance of MCP-1-positive cells. Few MCP-1-positive cells were observed in the thickened SMC at Day 35 in the CG group and the Tx-2 group (Figure 4A and C). MCP-1 positive cells were scattered over the whole interstitium at Day 35 in the Tx-1 group (Figure 4B). The number of MCP-1-positive cells was slightly increased in the Tx-1 group compared with that in the Tx-2 group (Figure 4D). The level of MCP-1 mRNA expression in the Tx-1 group was increased, but was not statistically significant (Figure 4E).

Appearance of vimentin-positive cells. Few vimentin-positive cells were observed in the SMC at Day 35 in the CG group and the Tx-2 group (Figure 5A and C). Vimentin-positive cells, which indicate mesenchymal cells, were scattered over the whole SMC at Day 35 in the Tx-1 group (Figure 5B). The number of vimentin-positive cells and the mRNA expression of vimentin in the Tx-1 group were also significantly higher compared with those in the CG and the Tx-2 group (Figure 5D and E).

mRNA expressions of EMT and RAS/MAP kinase at Day 35

After TSMCs transplantation at Day 22, mesenchymal cells were significantly increased in the peritoneum at Day 35. The level of mRNA expression of Snail in the Tx-1 group, which indicates EMT, was significantly higher than that in the CG
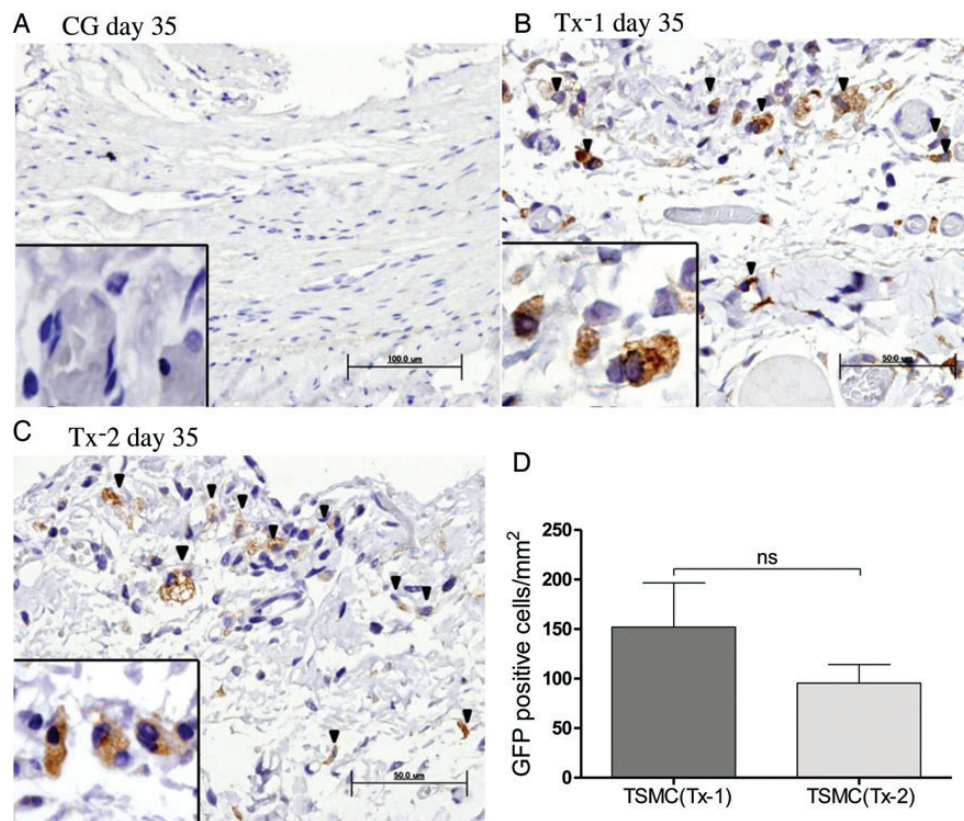
FIGURE 3: Appearance of GFP-positive TSMCs in the peritoneum (×400, *n* = 5 in each group). (**A**) Rat in the CG group at Day 35. (**B**) Rat in the Tx-1 group at Day 35. (**C**) Rat in the Tx-2 group at Day 35. (**D**) The number of GFP-positive cells in the Tx-1 group was almost similar with that in the Tx-2 group. Error bars represent SD.

group and Tx-2 group (Figure 6A). The levels of mRNA expression of B-Raf and MEK1 in the Tx-1 group, which are proteins in RAS/MAPK intercellular signal pathway, were higher than those in the CG group and Tx-2 group, but were not statistically significant (Figure 6B and C). The level of ERK1 mRNA expression in the Tx-1 group, which is proteins in the RAS/MAPK intercellular signal pathway, was significantly higher than that in the CG group and Tx-2 group (Figure 6D). The mRNA expressions of EMT and RAS/MAP kinase tended to be high in the Tx-1 group.

### Characteristics of infiltrating GFP-positive TSMCs in peritoneal interstitium at Day 35

At Day 35, many α-SMA positive cells were presented in the peritoneal interstitium (Figure 7A). Immunostaining with anti-GFP antibody was colocalized with immunostaining of anti-α-SMA antibody in the Tx-1 and Tx-2 group (Figure 7A). TGF-β expressing cells were also focused in the peritoneum at Day 35 (Figure 7B). Transplanted GFP-positive cells were expressed TGF-β in the Tx-1 rat. The GFP-negative surrounding cells were also expressed TGF-β as well as the transplanted GFP-positive cells in the Tx-1 rat. VEGF expressing cells were focused in the Tx-1 group at Day 35 (Figure 7C). Transplanted GFP-positive cells were expressed VEGF in the peritoneum. The GFP-negative surrounding cells were also expressed VEGF as well as the transplanted GFP-positive cells in the peritoneum.

DISCUSSION

In the present study, we observed that the thickening of peritoneal tissues was aggravated by TSMC transplantation under the over-production of TGF-β in the recipient peritoneum. And the levels of TGF-β, VEGF and MMP-2 mRNA expressions remained high, the transplanted mesothelial cells and the surrounding cells indicated the production of cytokines, such as TGF-β and VEGF by the TSMCs transplantation under the inflammation.

Previous reports have shown that a layer of transplanted mesothelial cells on a regenerated peritoneal surface is observed within 3 days in acute peritonitis animal models [20–22]. Hekking *et al.* [7, 20] also reported that some of the transplanted mesothelial cells were observed on the peritoneal membrane during peritoneal repair. They also reported that the transplanted mesothelial cells lead to peritoneal activation as an increase in the number of peritoneal lymphocytes and mast cells accompanied the induction of MCP-1 and hyaluronan in peritonitis rats [7]. In lung disease, the transplanted epithelial cells prevented bleomycin-induced lung injury and preserved lung function [23]. Mesothelial cell transplantation may make it possible to restore peritoneal injury, although there are few studies about the effect of mesothelial cell transplantation in PD.

In this study, the TSMCs were observed not on the surface of the peritoneum but in the thickened SMC in CG-induced
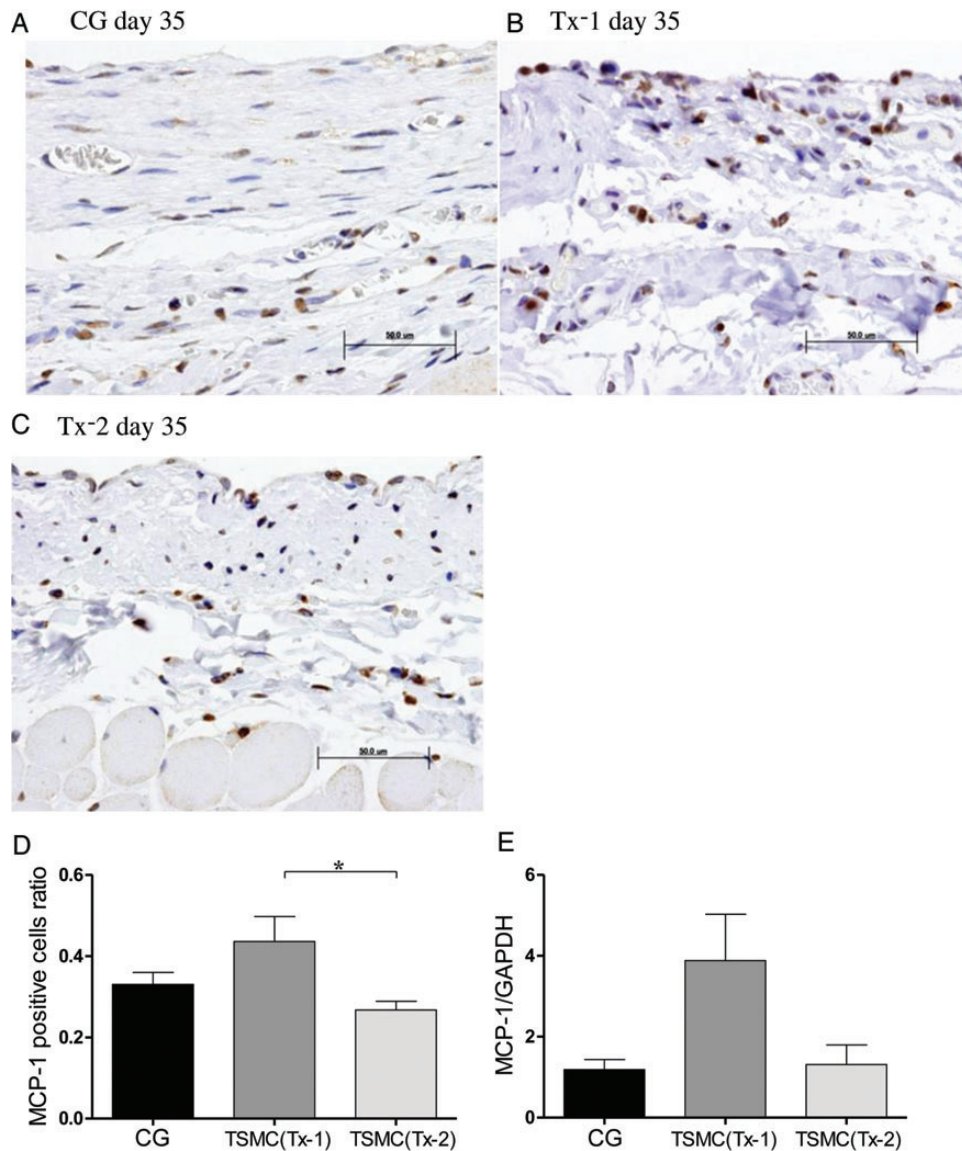
FIGURE 4: Appearance of MCP-1-positive cells in the peritoneum (×400, $n = 5$ in each group). (**A**) Rat in the CG group at Day 35. (**B**) Rat in the Tx-1 group at Day 35. (**C**) Rat in the Tx-2 group at Day 35. (**D**) MCP-1-positive cells in the Tx-1 group were slightly increasing than those in the Tx-2 group. The MCP-1 positive cells ratio = (MCP-1 positive cells/SMC mm^2 at day 35 in each group)/(MCP-1 positive cells/SMC mm^2 at day 22 in the CG group). (**E**) There were no significant changes of mRNA expression of MCP-1. Error bars represent SD.

peritoneal fibrosis rats. The damaged peritoneum was covered with a monolayer of flatted mesothelial cells both in the Tx-1 and Tx-2 groups at Day 35. Therefore, the transplanted TSMCs were not placed on the surface as mesothelial cells but play a role as an inducer of mesenchymal-epithelial transdifferentiation (MET). To determine the paracrine effect of transplanted mesothelial cells, we injected temperature-sensitive mesothelial cells, of which proliferation is controlled by temperature. The TSMCs were not proliferated but only differentiated at what might be an interperitoneal temperature of 38°C in the rats [15]. The characteristics of TSMCs might be one of the reasons for results to be different from previous reports [20–22]. As the transplanted cells play a different role between injury in acute and chronic stages, we examined the effect of

the cell transplantation using the damaged peritoneum caused by continuous CG injury.

Transplanted TSMCs in the SMC-modified tissue repair through the excretion of various cytokines and growth factors in response to their environment of peritoneal cavity in this study. Witkowicz [21] suggested that mesothelial cell transplantation has not yet been accepted as a method for damaged peritoneum restoration in PD patients for several reasons. Especially, the transplanted cells may enhance inflammation via an increased release of pro-inflammatory factors.

Mesothelial cells injected into peritoneal cavity were sustained, and the number of TSMCs was no different between the Tx-1 group and Tx-2 group in the peritoneum at Day 35. Some of the transplanted TSMCs in the thickened SMC were
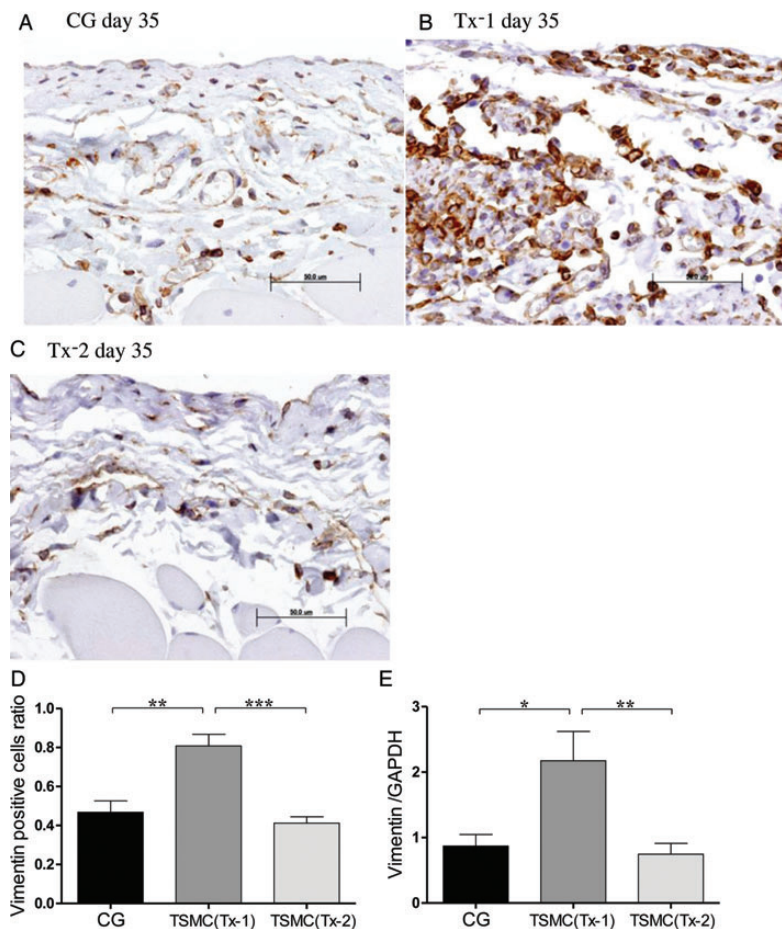
FIGURE 5: Appearance of vimentin-positive cells in the peritoneum (×400, $n = 5$ in each group). (**A**) Rat in the CG group at Day 35. (**B**) Rat in the Tx-1 group at Day 35. (**C**) Rat in the Tx-2 group at Day 35. (**D**) Vimentin-positive cells in the Tx-1 group were significantly increasing than those in the CG and Tx-2 group. The Vimentin positive cells ratio = (Vimentin positive cells/SMC mm^2 at day 35 in each group)/(Vimentin positive cells/SMC mm^2 at day 22 in the CG group). (**E**) The mRNA expression of vimentin in the Tx-1 group was significantly higher than in the CG and Tx-2 group. Error bars represent SD.
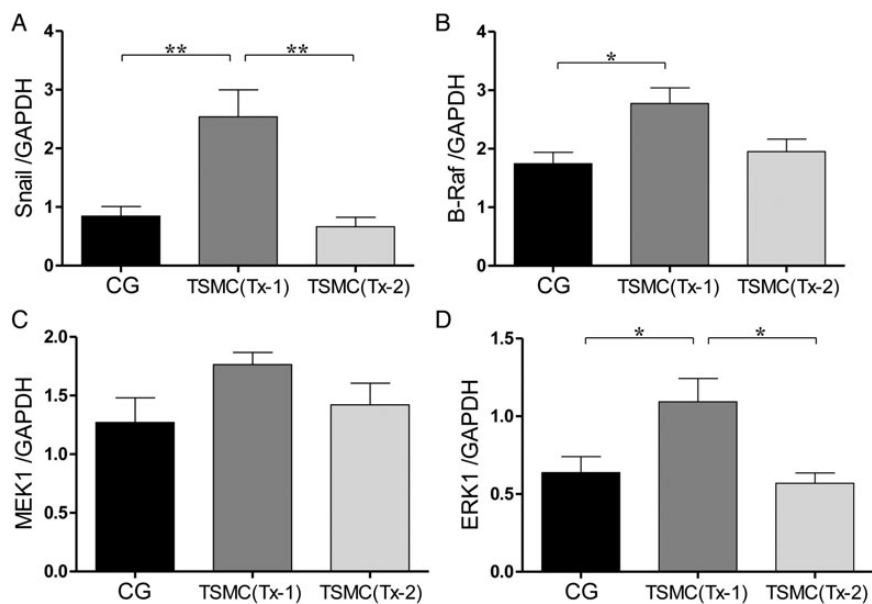
FIGURE 6: The level of mRNA expression such as EMT and RAS/MAP kinase at Day 35. (**A** and **B**) The mRNA expression of B-Raf and MEK1 was slightly high in the Tx-1 group. (**C** and **D**) The mRNA expression of ERK1 and Snail in the Tx-1 group was significantly higher than that in the CG and Tx-2 group. Error bars represent SD.
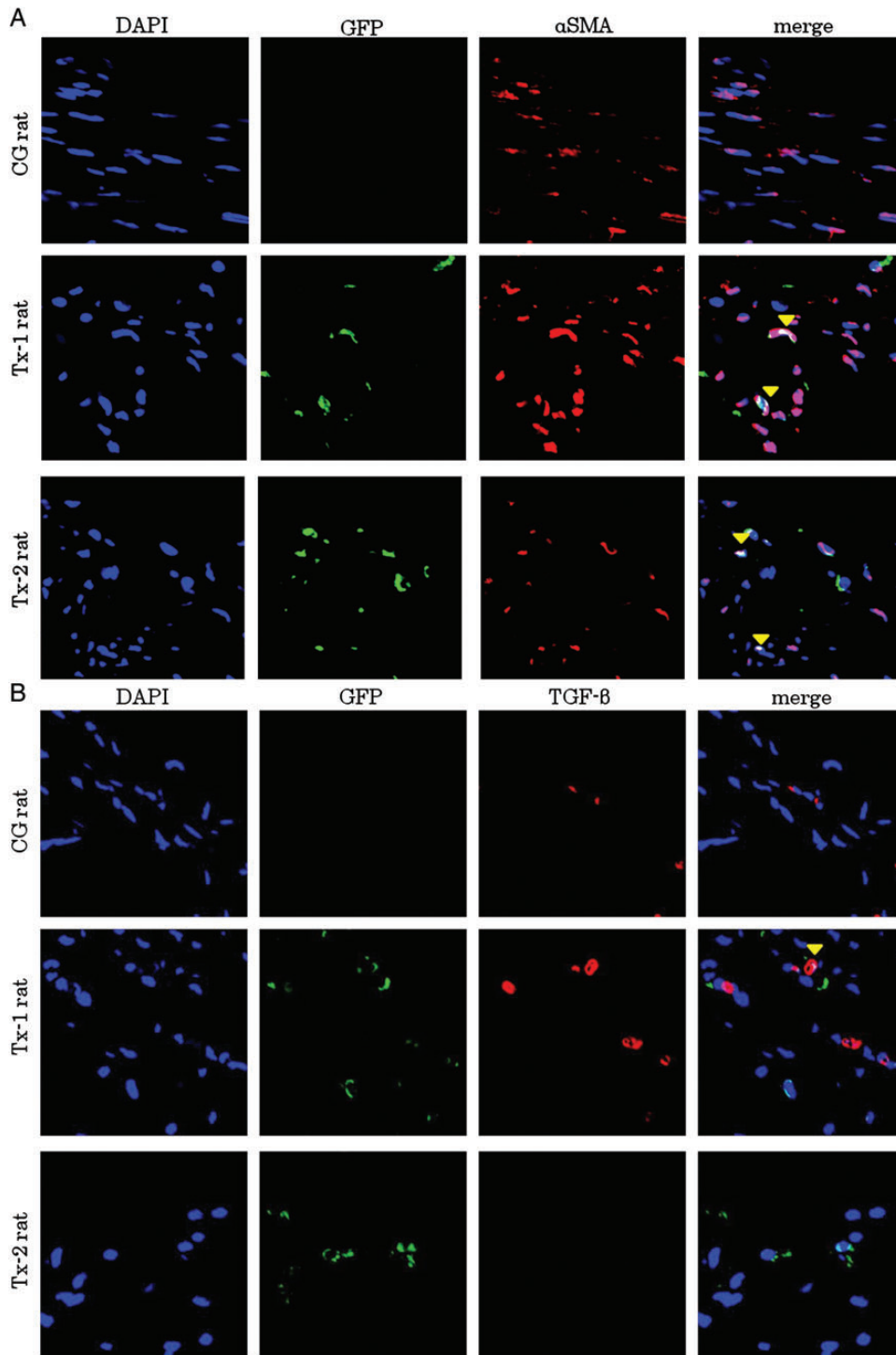
FIGURE 7: Characteristics of GFP-positive cells in the peritoneal interstitium at Day 35. Double immunofluorescence of GFP, α-SMA, TGF-β and VEGF antibodies. GFP-positive cells were enhanced by Alexa 488, α-SMA, TGF-β and VEGF-positive cells were enhanced by Alexa 555. The cell nuclei were labeled with a DAPI stain. (**A**) At Day 35, many α-SMA positive cells were observed in the peritoneal interstitium. Immunostaining with anti-GFP antibody was colocalized with immunostaining of anti-α-SMA antibody in the Tx-1 and Tx-2 groups. (**B**) TGF-β expressing cells were also focused in the peritoneum at day 35. Transplanted GFP-positive cells expressed TGF-β in the Tx-1 group. The GFP-negative surrounding cells were also expressed TGF-β as well as the transplanted GFP-positive cells in the Tx-1 group. (**C**) VEGF expressing cells were focused in the Tx-1 group at Day 35. Transplanted GFP-positive cells were expressed VEGF in the peritoneum. The GFP-negative surrounding cells were also expressed VEGF as well as the transplanted GFP-positive cells in the peritoneum.

expressed α-SMA as a maker of fibroblasts in the Tx-1 and Tx-2 groups. The SMC thickness at Day 35 in the Tx-2 group was similar to that of the CG group. The levels of TGF-β, VEGF, HGF, MMP-2 and PAI-1 mRNA expressions were not significantly different between the Tx-2 group and CG group at Day 35. It appears that the peritoneal fibrosis caused by CG
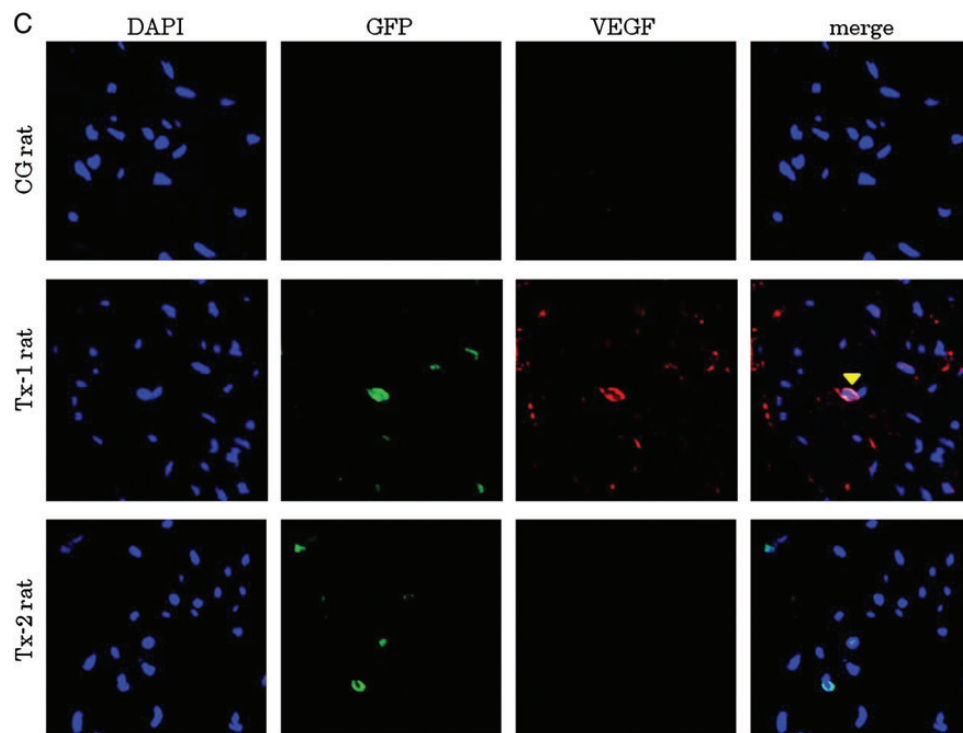
C

| | DAPI | GFP | VEGF | merge |

(rows labeled: CG rat, Tx-1 rat, Tx-2 rat)

exposure was not improved by the mesothelial transplantation at the healing stage. However, the mesothelial transplantation at the inflammatory phase aggravated peritoneal inflammation and tissue damage through increased release of pro-inflammatory factors, such as TGF-β and VEGF. The number of MCP-1 positive cell in Tx-1 was comparable with that in Tx-2, although transplanted TSMCs in the SMC were expressed α-SMA, as a maker of fibroblasts. The levels of TGF-β, VEGF and MMP-2 mRNAs were increased by mesothelial transplantation at the inflammatory phase. According to these results, it appears that the paracrine effects of transplanted mesothelial cells during peritoneal repair depend on the environment in the recipient's peritoneal cavity. Mesothelial cells have the potential to release various cytokines and growth factors, and also produce synthesize extracellular matrix components, as shown in previous research [12, 24–26]. Mesothelial cells derived from the mesoderm demonstrate phenotype features of both epithelial (of endodermal origin) and mesenchymal cells. A transdifferentiation of mesothelial cells to myofibroblasts has been reported when adding TGF-β to a culture of human mesothelial cells [27]. In this study, the TSMCs switched from mesothelial cells to fibroblasts showed not only phenotype, but also biological function. In this study, the TSMCs themselves expressed TGF-β and VEGF which induce fibrosis, chemotaxis and EMT. Furthermore, we clearly showed that the RAS/MAPK pathway was one of the processes whose transplanted TSMCs were transformed by the inflammation of recipient's peritoneal cavity. The Snail is a strong repressor of E-cadherin-mediated cell–cell adhesion. The Snail was activated through the RAS/MAPK pathway activation by the inflammation, such as the high level of TGF-β mRNA expression [13, 28, 29]. Peinado *et al.* [28] has reported that

TGF-β-mediated induction of the Snail transcription factor depends on both MAPK and phosphatidylinositol 3-kinase activities. The mediated factors, which were induced EMT through the effect of TGF-β on the Ras/MAPK pathway or cell proliferation, were not clear. A possibility is that the EMT induction effect of TGF-β actualized can be considered because the transplanted TSMCs were not proliferated but only differentiated in the peritoneum of the rats.

The purpose of this study was to clarify the paracrine effects of the transplanted mesothelial cells that synthesize cytokines and growth factors, and establish methods for the clinical therapy of mesothelial cells transplantation in PD patients. Although it was highlighted that the transplanted TSMCs under the inflammation were shown to aggravate the thickening of peritoneal tissues, the transplanted TSMCs during the recovery term of the inflammation were not shown to improve peritoneal wound healing. In this study, using continuous CG-induced peritoneal injury rats, the transplanted mesothelial cells were not observed on peritoneal membrane, but only on the thickened SMC. It is well known that mesothelial cells have the crucial role of anti-inflammatory and immunomodulatory properties through acute peritoneal injury. We should further examine the safety and efficacy of mesothelial cell transplantation for morphological and functional improvement, involving the number of injected mesothelial cells or the times which mesothelial cells are injected into the peritoneal cavity.

CONFLICT OF INTEREST STATEMENT

None declared.

REFERENCES

1. Chan TM, Leung JK, Tsang RC *et al*. Emodin ameliorates glucose-induced matrix synthesis in human peritoneal mesothelial cells. Kidney Int 2003; 64: 519–533

2. Topley N, Jorres A, Luttmann W *et al*. Human peritoneal mesothelial cells synthesize interleukin-6: induction by IL-1 beta and TNF alpha. Kidney Int 1993; 43: 226–233

3. Lee HB, Yu MR, Song JS *et al*. Reactive oxygen species amplify protein kinase C signaling in high glucose-induced fibronectin expression by human peritoneal mesothelial cells. Kidney Int 2004; 65: 1170–1179

4. Boulanger E, Wautier MP, Wautier JL *et al*. AGEs bind to mesothelial cells via RAGE and stimulate VCAM-1 expression. Kidney Int 2002; 61: 148–156

5. Yanez-Mo M, Lara-Pezzi E, Selgas R *et al*. Peritoneal dialysis and epithelial-to-mesenchymal transition of mesothelial cells. N Engl J Med 2003; 348: 403–413

6. Yung S, Chan TM. Intrinsic cells: mesothelial cells—central players in regulating inflammation and resolution. Perit Dial Int 2009; 29(Suppl. 2): S21–S27

7. Hekking LH, Zweers MM, Keuning ED *et al*. Apparent successful mesothelial cell transplantation hampered by peritoneal activation. Kidney Int 2005; 68: 2362–2367

8. Hoff CM, Shockley TR. Peritoneal dialysis in the 21st century: the potential of gene therapy. J Am Soc Nephrol 2002; 13(Suppl 1): S117–S124

9. Tomino Y. Mechanisms and interventions in peritoneal fibrosis. Clin Exp Nephrol 2012; 16: 109–114

10. Bertram P, Tietze L, Hoopmann M *et al*. Intraperitoneal transplantation of isologous mesothelial cells for prevention of adhesions. Eur J Surg 1999; 165: 705–709

11. Foley-Comer AJ, Herrick SE, Al-Mishlab T *et al*. Evidence for incorporation of free-floating mesothelial cells as a mechanism of serosal healing. J Cell Sci 2002; 115: 1383–1389

12. Offner FA, Feichtinger H, Stadlmann S *et al*. Transforming growth factor-beta synthesis by human peritoneal mesothelial cells. Induction by interleukin-1. Am J Pathol 1996; 148: 1679–1688

13. Strippoli R, Benedicto I, Perez Lozano ML *et al*. Epithelial-to-mesenchymal transition of peritoneal mesothelial cells is regulated by an ERK/NF-kappaB/Snail1 pathway. Dis Model Mech 2008; 1: 264–274

14. Sekiguchi Y, Zhang J, Patterson S *et al*. Rapamycin inhibits transforming growth factor beta-induced peritoneal angiogenesis by blocking the secondary hypoxic response. J Cell Mol Med 2012; 16: 1934–1945

15. Hotta Y, Kaneko K, Inuma J *et al*. Establishment of a peritoneal mesothelial cell line from a transgenic rat harbouring the temperature-sensitive simian virus 40 large T-antigen gene. Nephrol Dial Transplant 2010; 25: 1825–1832

16. Komatsu H, Uchiyama K, Tsuchida M *et al*. Development of a peritoneal sclerosis rat model using a continuous-infusion pump. Perit Dial Int 2008; 28: 641–647

17. Hayashi K, Kaufman L, Ross MD *et al*. Definition of the critical domains required for homophilic targeting of mouse sidekick molecules. FASEB J 2005; 19: 614–616

18. Honda K, Hamada C, Nakayama M *et al*. Impact of uremia, diabetes, and peritoneal dialysis itself on the pathogenesis of peritoneal sclerosis: a quantitative study of peritoneal membrane morphology. Clin J Am Soc Nephrol 2008; 3: 720–728

19. Shimaoka T, Hamada C, Kaneko K *et al*. Quantitative evaluation and assessment of peritoneal morphologic changes in peritoneal dialysis patients. Nephrol Dial Transplant 2010; 25: 3379–3385

20. Hekking LH, Harvey VS, Havenith CE *et al*. Mesothelial cell transplantation in models of acute inflammation and chronic peritoneal dialysis. Perit Dial Int 2003; 23: 323–330

21. Witkowicz J. Mesothelial cell transplantation. Pol Arch Med Wewn 2008; 118: 307–313

22. Di Paolo N, Vanni L, Sacchi G. Autologous implant of peritoneal mesothelium in rabbits and man. Clin Nephrol 1990; 34: 179–184

23. Murphy S, Lim R, Dickinson H *et al*. Human amnion epithelial cells prevent bleomycin-induced lung injury and preserve lung function. Cell Transplant 2011; 20: 909–923

24. Mandl-Weber S, Cohen CD, Haslinger B *et al*. Vascular endothelial growth factor production and regulation in human peritoneal mesothelial cells. Kidney Int 2002; 61: 570–578

25. Cronauer MV, Stadlmann S, Klocker H *et al*. Basic fibroblast growth factor synthesis by human peritoneal mesothelial cells: induction by interleukin-1. Am J Pathol 1999; 155: 1977–1984

26. Herrick SE, Mutsaers SE. Mesothelial progenitor cells and their potential in tissue engineering. Int J Biochem Cell Biol 2004; 36: 621–642

27. Yang AH, Chen JY, Lin JK. Myofibroblastic conversion of mesothelial cells. Kidney Int 2003; 63: 1530–1539

28. Peinado H, Quintanilla M, Cano A. Transforming growth factor beta-1 induces snail transcription factor in epithelial cell lines: mechanisms for epithelial mesenchymal transitions. J Biol Chem 2003; 278: 21113–21123

29. Margetts PJ. Twist: a new player in the epithelial-mesenchymal transition of the peritoneal mesothelial cells. Nephrol Dial Transplant 2012; 27: 3978–3981